

# Hematopoiesis specific loss of Cdk2 and Cdk4 results in increased erythrocyte size and delayed platelet recovery following stress

Senthil Raja Jayapal,<sup>1</sup> Chelsia Qiuxia Wang,<sup>1,2</sup> Xavier Bisteau,<sup>1</sup> Matias J. Caldez,<sup>1,3</sup> Shuhui Lim,<sup>1</sup> Vinay Tergaonkar,<sup>1</sup> Motomi Osato,<sup>2</sup> and Philipp Kaldis<sup>1,3</sup>

<sup>1</sup>Institute of Molecular and Cell Biology, A\*STAR Agency for Science, Technology and Research; <sup>2</sup>Cancer Science Institute of Singapore, National University of Singapore; and <sup>3</sup>National University of Singapore, Department of Biochemistry, Republic of Singapore

## ABSTRACT

Mouse knockouts of Cdk2 and Cdk4 are individually viable whereas the double knockouts are embryonic lethal due to heart defects, and this precludes the investigation of their overlapping roles in definitive hematopoiesis. Here we use a conditional knockout mouse model to investigate the effect of combined loss of Cdk2 and Cdk4 in hematopoietic cells. Cdk2<sup>fl/fl</sup>Cdk4<sup>-/-</sup>vavCre mice are viable but displayed a significant increase in erythrocyte size. Cdk2<sup>fl/fl</sup>Cdk4<sup>-/-</sup>vavCre mouse bone marrow exhibited reduced phosphorylation of the retinoblastoma protein and reduced expression of E2F target genes such as cyclin A2 and Cdk1. Erythroblasts lacking Cdk2 and Cdk4 displayed a lengthened G1 phase due to impaired phosphorylation of the retinoblastoma protein. Deletion of the retinoblastoma protein rescued the increased size displayed by erythrocytes lacking Cdk2 and Cdk4, indicating that the retinoblastoma/Cdk2/Cdk4 pathway regulates erythrocyte size. The recovery of platelet counts following a 5-fluorouracil challenge was delayed in Cdk2<sup>fl/fl</sup>Cdk4<sup>-/-</sup>vavCre mice revealing a critical role for Cdk2 and Cdk4 in stress hematopoiesis. Our data indicate that Cdk2 and Cdk4 play important overlapping roles in homeostatic and stress hematopoiesis, which need to be considered when using broad-spectrum cyclin-dependent kinase inhibitors for cancer therapy.

## Introduction

Cyclin-dependent kinases (Cdks) play important roles in proliferation and development,<sup>1,2</sup> and their activities are deregulated in several types of cancer.<sup>3</sup> Inhibition of Cdk activity as a therapeutic strategy against cancer has been an area of research interest for a long time despite the few clinical successes achieved.<sup>4,5</sup> One of the challenges in using broad spectrum Cdk inhibitors in cancer therapy is their presumably deleterious effects on normal tissues, in particular the rapidly proliferating cell types such as hematopoietic cells. Understanding the tissue specific effects of Cdk inhibition is essential for developing a framework to test and select chemical Cdk inhibitors that are therapeutically potent with minimal side-effects on normal tissues.

Knockout mouse models have proven useful in uncovering the general and tissue-specific functions of Cdks and their partner cyclins. Knockouts of Cdks that regulate the G1/S transition (Cdk2, Cdk4, and Cdk6) demonstrated that they were individually dispensable for cell proliferation but displayed tissue specific roles.<sup>6-10</sup> This led to investigation of double and triple mutants of Cdks which revealed their overlapping and unique functions.<sup>7,11,12</sup> Cdk2<sup>-/-</sup> mice are sterile but overtly normal,<sup>6,8</sup> while Cdk4<sup>-/-</sup> mice displayed reduced body size, spontaneous onset of diabetes, and sterility.<sup>9,10</sup> The combined loss of Cdk2 and Cdk4 led to embryonic lethality around E15 due to heart defects, demonstrating the overlapping roles of Cdk2 and Cdk4 in cardiac development.<sup>11</sup> Cdk2<sup>-/-</sup>Cdk4<sup>-/-</sup> mouse embryonic fibroblasts (MEFs) displayed

decreased proliferation rate, impaired S phase entry, and premature senescence,<sup>11</sup> all of which were rescued by the loss of the retinoblastoma protein (Rb).<sup>13</sup> E14.5 Cdk2<sup>-/-</sup>Cdk4<sup>-/-</sup> embryos are characterized by reduced fetal liver cellularity but the relative percentages of hematopoietic stem and progenitor cells were normal.<sup>11</sup> Importantly, the mid-gestation lethality of the Cdk2<sup>-/-</sup>Cdk4<sup>-/-</sup> embryos precludes the investigation of the loss of these Cdk activities in adult definitive hematopoiesis.

In this study, we conditionally ablated floxed Cdk2 in the hematopoietic cells of Cdk4<sup>-/-</sup> mice using Cre recombinase driven by the Vav1 guanine nucleotide exchange factor promoter (vavCre)<sup>14</sup> to generate Cdk2<sup>fl/fl</sup>Cdk4<sup>-/-</sup>vavCre (DKO) mice. The DKO mice were viable and displayed significantly enlarged erythrocytes under homeostatic conditions. Deletion of Rb rescued the increased size displayed by the DKO erythrocytes, illustrating the role of Cdk2/Cdk4/Rb pathway in regulating the erythrocyte size. Recovery of platelet counts following cytoablative stress was delayed in DKO mice. Our findings uncover important overlapping roles of Cdk2 and Cdk4 in both homeostatic and stress hematopoiesis.

## Methods

### Mouse generation and analysis

All mouse work was carried out with approved Institutional Animal Care and Use Committee protocols at the Biological Resource Centre mouse facility at Biopolis, Singapore. Cdk2<sup>fl/fl</sup> mice (*Online Supplementary Appendix* and *Online Supplementary Figure S1*) were

©2015 Ferrata Storti Foundation. This is an open-access paper. doi:10.3324/haematol.2014.106468

The online version of this article has a Supplementary Appendix.

Manuscript received on February 24, 2014. Manuscript accepted on January 21, 2015.

Correspondence: kaldis@imcb.a-star.edu.sg

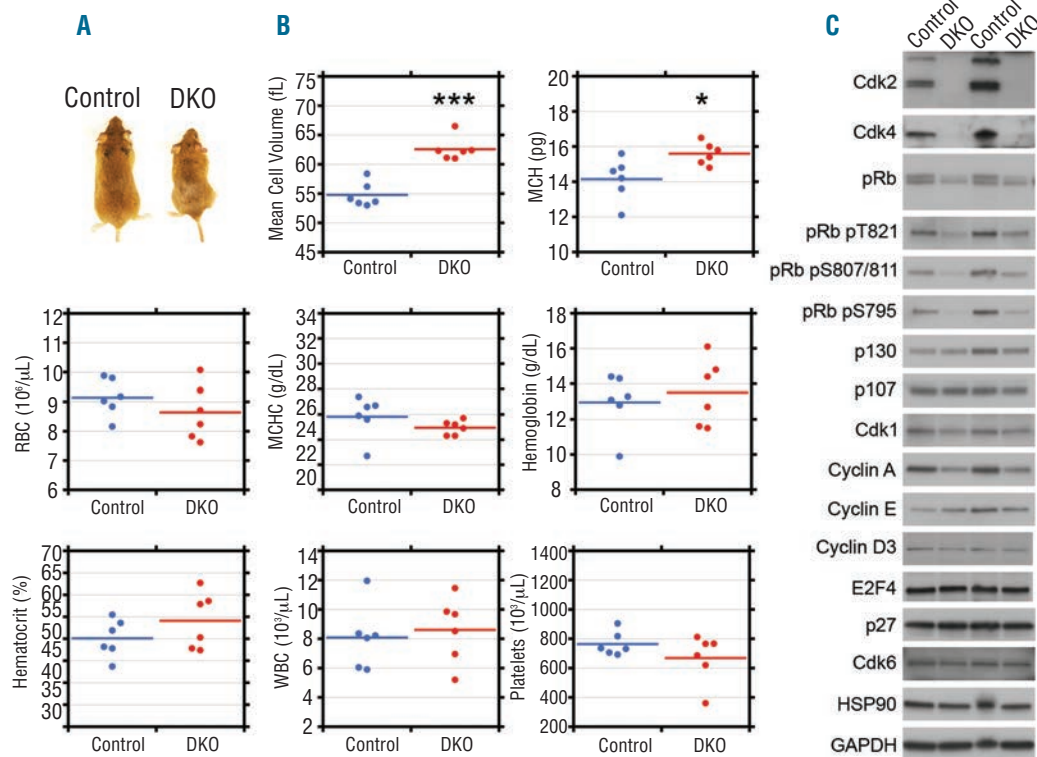


**Figure 1.** Cdk2 and Cdk4 regulate erythroid cell size. (A) Two-month old Cdk2<sup>fl/fl</sup>Cdk4<sup>-/-</sup>vavCre (DKO) and littermate wild-type (Control) mice are shown. (B) Complete blood count data for Cdk2<sup>fl/fl</sup>Cdk4<sup>-/-</sup>vavCre (DKO) mice (n=6) and littermate controls (n=6, wild-type or double heterozygotes) at two months of age. Two-tailed t-test results are indicated by asterisks; \**P*<0.05, \*\**P*<0.01, \*\*\**P*<0.001. (C) Western blot analysis of total bone marrow (BM) from 4-month old Cdk2<sup>fl/fl</sup>Cdk4<sup>-/-</sup>vavCre (DKO) and littermate Cdk2<sup>fl/fl</sup>Cdk4<sup>-/-</sup>vavCre or Cdk2<sup>fl/fl</sup>Cdk4<sup>-/-</sup>vavCre control mice (Control) with the indicated antibodies. HSP90 and GAPDH served as loading controls.

crossed with Cdk4<sup>+/-</sup> mice,<sup>10</sup> and the resulting heterozygous offspring Cdk2<sup>fl/fl</sup>Cdk4<sup>+/-</sup> were backcrossed with C57BL/6 mice to produce Cdk2<sup>fl/fl</sup>Cdk4<sup>+/-</sup> mice, which were in turn intercrossed to generate homozygous mutant Cdk2<sup>fl/fl</sup>Cdk4<sup>-/-</sup> mice. These mice were crossed with vavCre<sup>14</sup> mice to obtain Cdk2<sup>fl/fl</sup>Cdk4<sup>-/-</sup>vavCre (DKO) mice, which were in turn crossed to Rb<sup>fl/fl</sup> mice<sup>15</sup> to obtain Cdk2<sup>fl/fl</sup>Cdk4<sup>-/-</sup>Rb<sup>fl/fl</sup>vavCre (TKO) mice. Cdk2<sup>-/-</sup>Cdk4<sup>-/-</sup> embryos were obtained as previously described.<sup>11</sup> Cdk1<sup>fl/fl</sup> mice have been described previously.<sup>16</sup> The mice used in this study were of mixed C57BL/6 × 129S1/SvImJ background. Peripheral blood collected from the submandibular vein was used for complete blood count analysis using a Hemavet 950 FS hematology analyzer (Drew Scientific, CDC-9950-005).

### Stress hematopoiesis studies

To study the hematocrit recovery after stress, phenylhydrazine (Sigma, 114715) was dissolved at 6 mg/mL in sterile phosphate buffered saline (PBS) and injected intraperitoneally at 60 mg/kg on two consecutive days (D0 and D1). Peripheral blood was collected from the submandibular vein on D0, D2, D4, D7, and D10 to analyze the hematocrit recovery kinetics using a MEK-6318K Hematology Analyzer (Nihon Kohden). 5-fluorouracil (Sigma, F6627) solution in sterile water (5 mg/mL) was administered at a dose of 150 mg/kg intraperitoneally on D0 to study the recovery kinetics of hematocrit, white blood cells (WBC) counts, and platelet counts following cytoablative stress.

### Purification, culture and flow cytometry analysis of fetal liver erythroid progenitors

Fetal livers were isolated from E13.5 Cdk2<sup>-/-</sup>Cdk4<sup>-/-</sup> and litter-

mate control embryos, followed by purification and culture of TER119-negative, CD11b-negative erythroid progenitors as previously described.<sup>17</sup> The purified TER119-negative erythroblasts were seeded in fibronectin-coated plates and cultured in erythroid differentiation medium consisting of Iscove's modified Dulbecco medium (Gibco, 12440-053) containing 15% FBS (StemCell Technologies, 06200), 1% detoxified bovine serum albumin (StemCell Technologies, 09300), 200 µg/mL holo-transferrin (Sigma, T0665), 10 µg/mL recombinant human insulin (Sigma, 91077C), 2 mM L-glutamine (Invitrogen), 10<sup>-4</sup>M β-mercaptoethanol (Invitrogen), and 2 U/mL erythropoietin (R&D systems). Flow cytometry analysis of erythroid differentiation and enucleation was performed at 48 h in culture, as previously described.<sup>17</sup> For cell cycle analysis of fetal liver erythroblasts, total fetal liver cells freshly isolated from E13.5 embryos were fixed and permeabilized using the BD Cytotfix/Cytoperm™ Plus Fixation/Permeabilization Kit (BD Biosciences, 555028), stained with fluorophore-conjugated antibodies against TER119 and CD71, and incubated in PBS containing 10 µg/mL Hoechst 33342 (Invitrogen, H3570) and 200 µg/mL RNase A (Invitrogen, 12091-021) for 30 min at room temperature prior to FACS analysis on BD LSRII (BD Biosciences). FACS data were analyzed with FlowJo 7.5.5 software.

### Statistical analysis

Student's *t*-test was used to determine the significance of differences between treated samples and controls. Statistical analysis was performed using Microsoft Office Excel 2007.

For a detailed description of the materials and methods used, see the *Online Supplementary Appendix*.

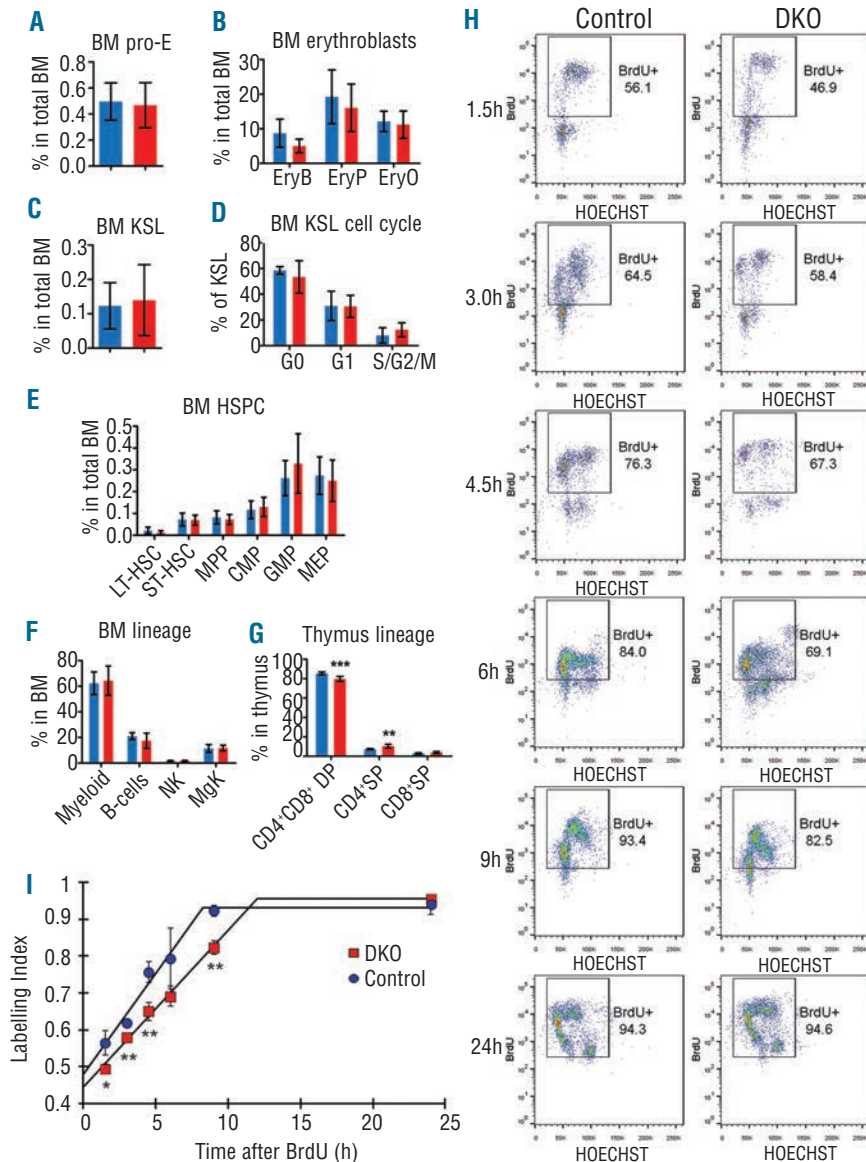


**Figure 2.** Analysis of hematopoietic stem and progenitor cells (HSPCs) in  $Cdk2^{fl/fl}Cdk4^{-/-}vavCre$  (DKO) mice. Flow cytometric analysis of HSPCs in  $Cdk2^{fl/fl}Cdk4^{-/-}vavCre$  DKO mice (red bars) and wild-type or double heterozygote  $Cdk2^{fl/fl}Cdk4^{fl/fl}vavCre$  littermate controls (blue bars). (A) Bone marrow (BM) frequency of  $CD71^{hi}TER119^{lo}$  pro-erythroblasts (pro-E) (n=4). (B) BM frequency of  $TER119^{hi}CD71^{hi}FSC^{hi}$  basophilic erythroblast (EryB),  $TER119^{hi}CD71^{hi}FSC^{lo}$  polychromatic erythroblast (EryP) and  $TER119^{hi}CD71^{lo}FSC^{lo}$  orthochromatic erythroblast (EryO) (n=4). (C) Frequency of c-Kit<sup>+</sup>Sca-1<sup>+</sup>Lineage<sup>+</sup> hematopoietic stem/progenitor cell (HSPC) compartment in the BM (n=5). (D) Flow cytometry analysis of Ki-67 expression in KSL cells. Percentage of KSL cells in the various cell cycle phases is shown (n=4). (E) BM frequencies of individual HSPC compartments (n=6). LT-HSC, ST-HSC and MPP compartments are gated from viable c-Kit<sup>+</sup>Sca-1<sup>+</sup>Lineage<sup>+</sup> (KSL) cells. CMP, GMP and MEP compartments are gated from viable c-Kit<sup>+</sup>Sca-1<sup>+</sup>Lineage<sup>+</sup> cells. CLP compartment are gated from viable c-Kit<sup>low</sup>Sca-1<sup>low</sup>Lineage<sup>+</sup> cells. LT-HSC: long-term hematopoietic stem cell; ST-HSC: short-term hematopoietic stem cell; MPP: multipotent progenitor; CMP: common myeloid progenitor; GMP: granulocyte/macrophage progenitor; MEP: megakaryocyte/erythroid progenitor; CLP: common lymphoid progenitor. (F) BM frequencies of indicated lineage cells (n=4). Myeloid: Mac-1<sup>+</sup> and Gr-1<sup>+</sup>; B cells: B220<sup>+</sup>CD19<sup>+</sup>; natural killer (NK) cells: CD3-Dx5<sup>+</sup>; megakaryocyte (MgK): CD41<sup>+</sup>CD61<sup>+</sup>. (G) Frequency of indicated lineage cells in the thymus (n=6). DP: double positive T cell; SP: single positive T cell. (H and I) Bone marrow samples from  $Cdk2^{fl/fl}Cdk4^{-/-}vavCre$  mice (DKO) or from littermate controls (Control) were labeled with BrdU in culture for the indicated time periods (n=3). (H) The percentage of BrdU<sup>+</sup> CD71<sup>+</sup> erythroblasts (labeling index) are indicated. (I) The plot of BrdU labeling index of CD71<sup>+</sup> bone marrow erythroblasts versus the cumulative BrdU labeling time is shown. Error bars represent standard deviation. Two-tailed t-test results are indicated by asterisks; \* $P < 0.05$ , \*\* $P < 0.01$ , \*\*\* $P < 0.001$ .

## Results

$Cdk2^{fl/fl}Cdk4^{-/-}vavCre$  (DKO) mice were viable, displayed smaller body size (Figure 1A), and presented sterility similar to  $Cdk4^{-/-}$  mice.<sup>9,10</sup> DKO mice constituted 5% of the total mice genotyped at weaning age (n=517), which is less than the expected Mendelian ratio for the complete linkage of the  $Cdk2$  and  $Cdk4$  locus (12.5%) due to frequent unlinking of the  $Cdk2$  and  $Cdk4$  loci in the pups. To analyze hematopoiesis, we determined complete blood counts of the DKO mice, which revealed a significant increase in erythrocyte mean cell volume (average  $MCV=62.6$  fl) and a resultant slight increase in mean cell hemoglobin (average  $MCH=15.6$  pg), compared to littermate controls (average  $MCV=54.8$  fl, average  $MCH=14.2$  pg) (Figure 1B). Hence combined loss of  $Cdk2$  and  $Cdk4$  in hematopoietic cells leads to increased erythrocyte size, unlike the normal erythrocyte size displayed by the single knockouts  $Cdk2^{-/-6}$  ( $MCV=56\pm 0.3$  fl; n=3) or  $Cdk4^{-/-10}$

( $MCV=56.1\pm 0.65$  fl; n=3). The DKO mice showed no significant changes in the other peripheral blood parameters analyzed. Western blot analysis of DKO bone marrow lysates confirmed the absence of  $Cdk2$  and  $Cdk4$  proteins (Figure 1C). Rb phosphorylation was significantly decreased in the DKO bone marrow. We had previously shown that, during late stage embryogenesis, Rb phosphorylation requires  $Cdk2$  or  $Cdk4$  but other kinases can phosphorylate Rb before E14.<sup>11</sup> Hence Rb phosphorylation in adult bone marrow also requires  $Cdk2$  or  $Cdk4$ , revealing an important overlapping function for these Cdks in adult mice. The levels of the other pocket proteins, p107 and p130, remained unchanged. Consistent with the decreased Rb phosphorylation, the expression of E2F target genes such as  $Cdk1$  and cyclin A2 was significantly decreased in the DKO bone marrow. There were no significant alterations in levels of cyclin D3 and E2F4, proteins that have been implicated in regulating erythrocyte size.<sup>18-21</sup> The levels of  $Cdk6$ , cyclin E, and the Cdk inhibitor

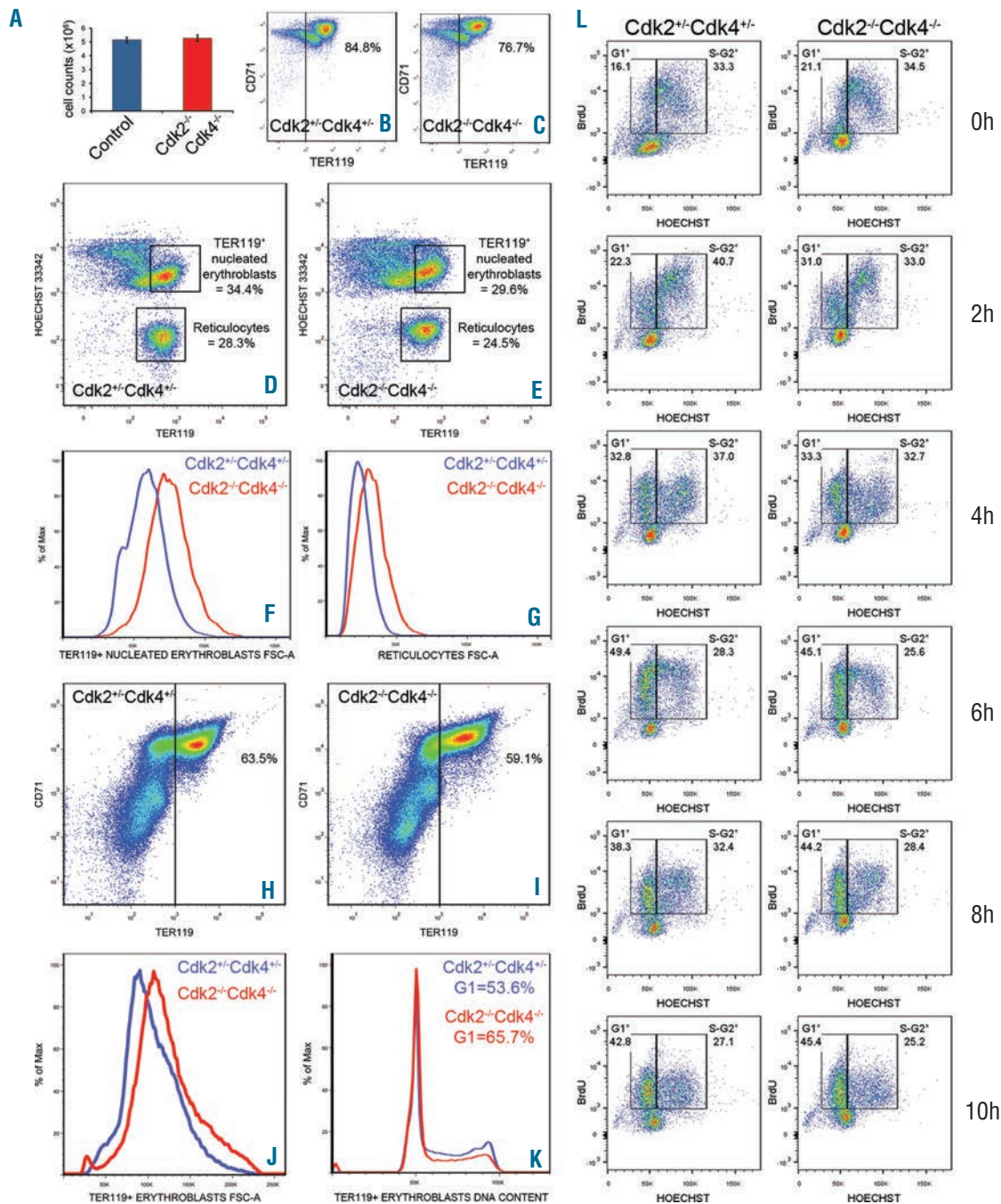


**Figure 3.** Analysis of fetal liver erythroblasts lacking Cdk2 and Cdk4. (A-G) TER119<sup>+</sup> fetal liver erythroblasts were purified from  $Cdk2^{-/-}Cdk4^{-/-}$  and littermate control ( $Cdk2^{-/-}Cdk4^{+/+}$  or  $Cdk2^{+/+}Cdk4^{+/+}$ ) E13.5 mouse embryos and cultured in erythropoietin-containing medium in fibronectin-coated plates for 48 h, followed by cell counting and FACS analysis. (A) Total cell counts at 48 h in culture for an equal starting cell number ( $5 \times 10^5$ ) of TER119<sup>+</sup> fetal liver erythroblasts. Error bars represent standard deviation ( $n=3$ ). Two-tailed t-test results are indicated by asterisks; \* $P < 0.05$ , \*\* $P < 0.01$ , \*\*\* $P < 0.001$ . (B and C) Erythroid differentiation was assayed after 48 h in culture by quantifying the CD71<sup>+</sup>TER119<sup>+</sup> population, which represents the late stage erythroid cells. (D and E) Enucleation was assayed by quantifying the TER119<sup>+</sup>HOECHST<sup>-</sup>reticulocyte populations, which correspond to the enucleated reticulocytes. (F and G) Forward scatter histogram overlays of HOECHST<sup>+</sup>TER119<sup>+</sup> (TER119<sup>+</sup> nucleated erythroblasts) and TER119<sup>+</sup>HOECHST<sup>-</sup> (Reticulocytes) erythroblast populations gated as shown in (D) and (E). (H-K) Total fetal liver cells isolated from  $Cdk2^{-/-}Cdk4^{-/-}$  and littermate control ( $Cdk2^{-/-}Cdk4^{+/+}$  or  $Cdk2^{+/+}Cdk4^{+/+}$ ) E13.5 mouse embryos were fixed, permeabilized, and immunostained for CD71 and TER119, followed by staining with HOECHST 33342 and RNase A treatment. (H and I) The TER119 versus CD71 immunophenotyping profiles for the fetal liver cells, and the fraction of gated TER119<sup>+</sup> populations are shown. (J) Forward scatter histogram overlays of TER119<sup>+</sup> fetal liver erythroblasts gated as shown in panels (H) and (I). (K) DNA content histogram (HOECHST 33342 staining) overlays of TER119<sup>+</sup> fetal liver erythroblasts gated as shown in (H) and (I). The fraction of cells in the G1 phase of the cell cycle is indicated. (L) TER119<sup>+</sup> fetal liver erythroblasts were purified from  $Cdk2^{-/-}Cdk4^{-/-}$  and littermate control ( $Cdk2^{-/-}Cdk4^{+/+}$  or  $Cdk2^{+/+}Cdk4^{+/+}$ ) E13.5 mouse embryos ( $n=4$ ), and cultured in erythropoietin-containing medium for 12 h, followed by a 1 h BrdU pulse (10  $\mu$ M). After 1 h BrdU pulsing, the cells were washed to remove the BrdU and cultured again in erythropoietin-containing medium. Cells were harvested at the indicated time points for fixing and staining for BrdU. A representative data set of BrdU versus HOECHST FACS plots is shown. The percentage of BrdU-labeled G1-phase and BrdU-labeled S/G2/M phase cells are indicated as G1\* and S-G2\*, respectively.

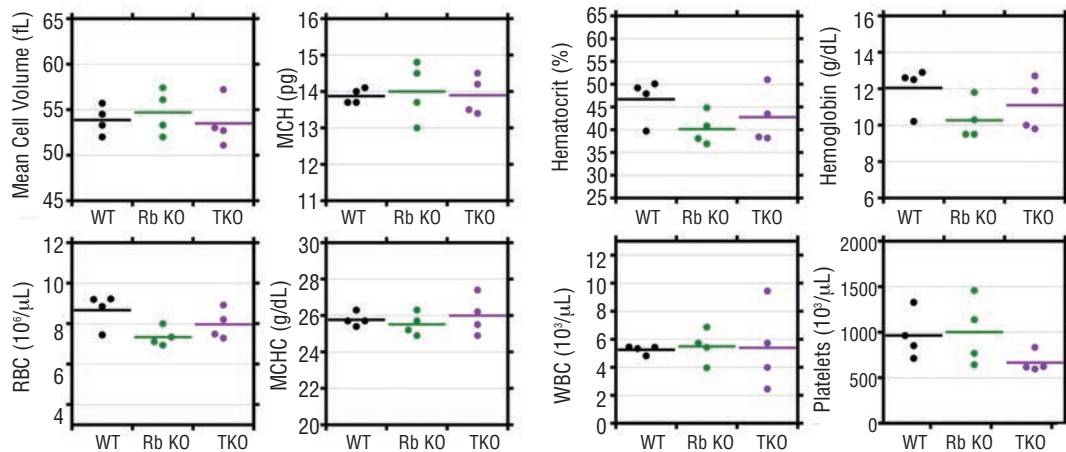


**Figure 4.** Deletion of Rb rescued the increased erythrocyte size observed in  $Cdk2^{fl/fl}Cdk4^{-/-}vavCre$  (DKO) mice. Complete blood count data from age-matched  $Cdk2^{fl/fl}Cdk4^{-/-}Rb^{fl/fl}vavCre$  (TKO),  $Rb^{fl/fl}vavCre$  (Rb KO), and wild-type control mice ( $n=4$ ). Two-tailed t-test results are indicated by asterisks; \* $P<0.05$ , \*\* $P<0.01$ , \*\*\* $P<0.001$ .

p27 also remained unchanged. In summary, the DKO mice display significantly enlarged erythrocytes without any signs of accompanying anemia, but the DKO bone marrow displayed reduced Rb phosphorylation and decreased expression of E2F target genes such as cyclin A2 and Cdk1.

Since the hematopoietic impairments in DKO mice were erythroid specific, we checked the bone marrow erythroblast populations (Figure 2A and B) but no significant changes were detected in their relative proportions. We also investigated the hematopoietic stem and progenitor cell fractions in the bone marrow defined by the marker combination  $c-kit^+Sca-1^+Lineage^-$  (KSL). The frequency (Figure 2C) and cell cycle phase distribution (Figure 2D) of the KSL population were unaffected in the DKO mice. The frequency of the various hematopoietic stem and progenitor cell (HSPCs) populations (Figure 2E), as well as those of more mature lineages (Figure 2F), were not affected in the DKO bone marrow. The cell cycle distribution of total bone marrow cells (*Online Supplementary Figure S2A*) and lineage restricted progenitor cells (*Online Supplementary Figure S2B-E*) were not significantly altered in DKO mice. The thymus displayed a slight decrease in the  $CD4^+CD8^+$  double positive population, and a slight increase in the  $CD4^+$  single positive population (Figure 2G). Hence no significant changes in DKO bone marrow HSPCs were detectable that could be linked to the increased erythrocyte size.

Since the frequencies of various erythroblast subpopulations were unchanged in DKO bone marrow (Figure 2A and B), we next investigated the erythroblast cell cycle. During terminal differentiation, erythroblasts undergo approximately 4-5 rapid cell divisions accompanied by a progressive decrease in cell size, followed by exit from the cell cycle.<sup>22</sup> The decrease in erythroblast size during terminal maturation divisions has been attributed to the loss or alteration of the cell size control at the G1-S restriction point leading to the shortening of the G1 phase of the cell cycle without changes to the length of S and G2/M phase.<sup>23</sup> To investigate changes in cell cycle time and G1 length in erythroblasts, we measured the length of various cell cycle phases in adult DKO mice bone marrow erythroblasts by cumulative BrdU labeling of bone marrow

cells in culture (Figure 2H and I). The cell cycle time ( $T_c$ ) and the length of S-phase ( $T_s$ ) were calculated using the Nowakowski method.<sup>24</sup> The cell cycle time for  $CD71^+$  bone marrow erythroblasts was increased in DKO (22.4 h) compared to that of littermate controls (16.9 h). The length of S phase (10.4 h in DKO vs. 8.7 h in control) as well as the length of G1+G2+M (12 h in DKO vs. 8.3 h in control) was markedly increased in the DKO erythroblasts, consistent with the critical roles for Cdk2 and Cdk4 in the G1-S transition. The increased cell cycle time of DKO erythroblasts indicates that a decrease in erythroblast proliferation *in vivo* cannot be ruled out, despite the normal erythrocyte counts (Figure 1B) and bone marrow erythroblast frequencies (Figure 2A and B) displayed by the DKO mice. Since the G2/M phase of cell cycle in erythroblasts is relatively short,<sup>23</sup> increased length of G1+G2+M is indicative of a longer G1 phase in DKO erythroblasts. This suggests that erythroblasts lacking Cdk2 and Cdk4 take longer to transit through the cell cycle and spend a longer time in the G1 phase. Since the reduction in erythroid cell size during terminal differentiation is regulated by the shortening of the G1 phase of the cell cycle without changes to the length of S and G2/M phases,<sup>25</sup> our data indicate that the increase in G1 length as well as total cell cycle time of erythroblasts lacking Cdk2 and Cdk4 are likely to lead to the enlarged erythrocyte size.

We next investigated the effect of combined loss of Cdk2 and Cdk4 on fetal liver erythropoiesis. We assayed the *in vitro* proliferation and differentiation of fetal liver erythroid progenitors obtained from E13.5  $Cdk2^{-/-}Cdk4^{-/-}$  embryos<sup>11</sup> using a well characterized *in vitro* culture system that mimics the terminal erythropoiesis *in vivo*.<sup>17,25,26</sup> No significant defects in proliferation (Figure 3A), terminal differentiation, or enucleation (Figure 3B-E) were detected in  $Cdk2^{-/-}Cdk4^{-/-}$  erythroblasts. The cell size distribution of the cultured  $Cdk2^{-/-}Cdk4^{-/-}$  erythroblasts was assayed by forward scatter (Figure 3F and G) of specific subpopulations gated in the TER119 *versus* Hoechst dot plots (Figure 3D and E). The Hoechst<sup>+</sup>TER119<sup>+</sup> fraction of erythroblasts represent the TER119<sup>+</sup> nucleated erythroblasts that subsequently undergo enucleation to give rise to the TER119<sup>+</sup>Hoechst<sup>-</sup> reticulocytes. If the increased erythro-

cyte size was the result of erythroblasts exiting the cell cycle earlier with fewer cell divisions, only the reticulocytes, but not the TER119<sup>+</sup> nucleated erythroblasts, should display an increased cell size. Nevertheless, both TER119<sup>+</sup> nucleated erythroblasts (Figure 3F) and the reticulocytes (Figure 3G) display increased cell size, suggesting that the increased erythrocyte size in the absence of Cdk2 and Cdk4 is not due to lower number of erythroblast cell divisions. We also assayed the cell size and cell cycle distribution of the TER119<sup>+</sup> erythroblasts *in vivo*, using total fetal

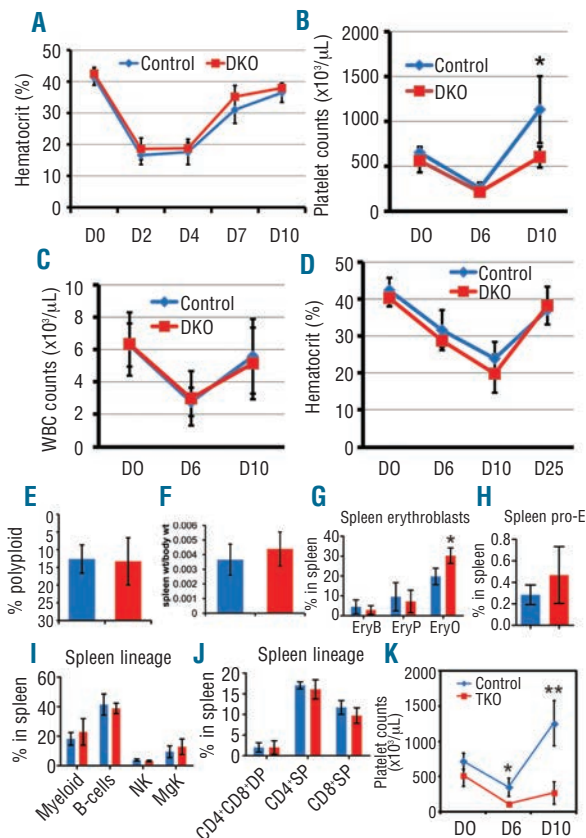


**Figure 5.** Stress hematopoiesis in Cdk2<sup>fl/fl</sup>Cdk4<sup>-/-</sup>vavCre mice. (A) Hematocrit recovery kinetics after PHZ treatment for Cdk2<sup>fl/fl</sup>Cdk4<sup>-/-</sup>vavCre (DKO) mice and age-matched control mice (n=6). (B-D) Hematopoietic recovery in Cdk2<sup>fl/fl</sup>Cdk4<sup>-/-</sup>vavCre (DKO) mice and littermate control mice (n=5) after a 5-fluorouracil challenge. Platelet counts (B), white blood cell counts (C), and hematocrit (D), on the indicated days after 5-fluorouracil treatment are shown. (E) Polyploidy analysis of megakaryocytes derived from Lineage-bone marrow cells from DKO mice (red bar) or littermate control mice (blue bar) cultured *in vitro* for three days (n=4). The percentage of CD41<sup>+</sup> cells with DNA content over 4n is shown. (F) The ratio of spleen weight to carcass weight for DKO mice (red bar) and littermate control mice (blue bar) is shown (n=6). (G-J) Flow cytometry analysis of hematopoietic cells in the spleen of Cdk2<sup>fl/fl</sup>Cdk4<sup>-/-</sup>vavCre (DKO) mice (red bars) and littermate control mice (blue bars). (G) Frequency of TER119<sup>hi</sup>CD71<sup>hi</sup>FSC<sup>hi</sup> basophilic erythroblast (EryB), TER119<sup>hi</sup>CD71<sup>hi</sup>FSC<sup>lo</sup> polychromatic erythroblast (EryP) and TER119<sup>hi</sup>CD71<sup>lo</sup>FSC<sup>lo</sup> orthochromatic erythroblast (EryO) in spleen (n=4). (H) Frequency of CD71<sup>hi</sup>TER119<sup>lo</sup> pro-erythroblasts (pro-E) in spleen is shown (n=4). (I) Frequency of cells of the indicated lineages in the spleen are shown (n=4). Myeloid: Mac-1<sup>+</sup> and Gr-1<sup>+</sup>; B cells: B220<sup>+</sup> CD19<sup>+</sup>; natural killer (NK) cells: CD3-Dx5<sup>+</sup>; megakaryocyte (MgK): CD41<sup>+</sup>CD61<sup>+</sup>. (J) Frequency of the indicated T-cell subtypes are shown (n=6). DP: double positive T cell; SP: single positive T cell. (K) Recovery of platelet counts following a 5-fluorouracil challenge in Cdk2<sup>fl/fl</sup>Cdk4<sup>-/-</sup>Rb<sup>fl/fl</sup>vavCre (TKO) and age-matched wild-type control mice (Control) (n=4). Error bars represent standard deviation. Two-tailed *t*-test results are indicated by asterisks; \**P*<0.05, \*\**P*<0.01, \*\*\**P*<0.001.

liver cells isolated from E13.5 embryos (Figure 3H-K). While the fraction of TER119<sup>+</sup> erythroblasts in the fetal liver was normal (Figure 3H and I), the Cdk2<sup>-/-</sup>Cdk4<sup>-/-</sup> TER119<sup>+</sup> erythroblasts displayed larger cell size (Figure 3J) as well as an increased G1 population (Figure 3K). To check whether this increased G1 population is indicative of slower transition through G1 phase, we performed BrdU pulse-chase experiments in fetal liver erythroblasts in culture (Figure 3L). The progression of DKO erythroblasts through the cell cycle was broadly similar to that of controls except for a mild increase in G1 population for most of the time points assayed (Figure 3L). This was consistent with the lack of proliferation defects in Cdk2<sup>-/-</sup>Cdk4<sup>-/-</sup> erythroblasts in culture (Figure 3A). Hence, loss of Cdk2 and Cdk4 has a modest effect on the fetal liver erythroblast cell cycle, compared to their significant effect on adult bone marrow erythroblasts.

The increased length of the G1 phase observed in bone marrow erythroblasts lacking Cdk2 and Cdk4 is most likely due to hypophosphorylation of Rb (Figure 1C), since Rb is a critical gatekeeper for the transition from G1 to S phase of the cell cycle.<sup>27,28</sup> Taken together, our data support a model where hyperphosphorylation and degradation of Rb requires the presence of either Cdk2 or Cdk4, with the combined deletion of both kinases promoting the repressive state of Rb, impairing the G1-S transition causing cells to spend a longer time in the G1 phase, ultimately resulting in increased cell size. To test this model, we investigated whether deletion of Rb could rescue the defects observed in the DKO mice. We had previously shown that loss of Rb rescued the proliferation defects in Cdk2<sup>-/-</sup>Cdk4<sup>-/-</sup> MEFs but did not rescue the lethality at mid-gestation of Cdk2<sup>-/-</sup>Cdk4<sup>-/-</sup> embryos.<sup>13</sup> Hence, we generated the Cdk2<sup>fl/fl</sup>Cdk4<sup>-/-</sup>Rb<sup>fl/fl</sup>vavCre (TKO) mice. The TKO mice were viable, demonstrating the surprising flex-

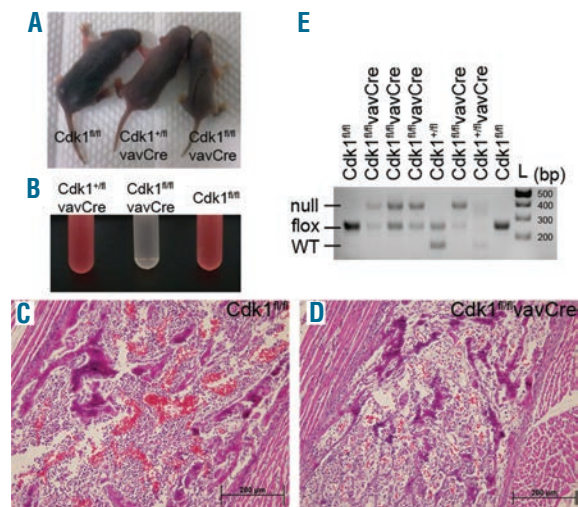


**Figure 6.** Cdk1<sup>fl/fl</sup>vavCre mice exhibit neonatal lethality due to hematopoietic failure. (A) Postnatal day 4 Cdk1<sup>fl/fl</sup>vavCre and littermate control mice. (B) Peripheral blood collected from facial veins of the mice shown in (A) and diluted 1000-fold in phosphate buffered saline (PBS). (C and D) Hematoxylin & Eosin stained bone marrow sections of postnatal day 1 littermate control Cdk1<sup>fl/fl</sup> (C) and Cdk1<sup>fl/fl</sup>vavCre (D) mice. (E) Genotyping of peripheral blood collected from postnatal day 1 mice resulting from a cross between Cdk1<sup>fl/fl</sup>vavCre female and Cdk1<sup>fl/fl</sup> male mice.

ibility in the mammalian hematopoietic system to adapt to the loss of key cell cycle regulators such as Cdk2, Cdk4, and Rb, without the loss of viability. The TKO mice displayed erythrocyte size (average MCV=53.5 fl; n=4) similar to wild-type (average MCV=53.9 fl; n=4) and Rb<sup>fl/fl</sup>vavCre (Rb KO, average MCV=54.7 fl; n=4) mice (Figure 4), indicating a rescue of the enlarged erythrocyte size displayed by DKO mice (average MCV=62.58 fl) (Figure 1B). Hence, deletion of Rb rescued the size of erythrocytes lacking Cdk2 and Cdk4, revealing an important role for the Cdk2/Cdk4/Rb pathway in regulating erythrocyte size.

Since homeostatic hematopoiesis was not majorly affected in the DKO mice, we aimed to investigate the hematopoietic recovery after stress. Recovery of the hematocrit in DKO mice after phenylhydrazine-induced hemolytic anemia was similar to age-matched controls (Figure 5A). Nevertheless, upon a 5-fluorouracil challenge (which destroys all proliferating cells), the recovery of platelet counts was significantly delayed in DKO mice compared to littermate controls (Figure 5B), while the WBC counts (Figure 5C) and hematocrit (Figure 5D) recovered normally. Since the megakaryocyte counts in DKO mice bone marrow were normal (Figure 2F), we checked for defects in polyploidization of megakaryocytes in the DKO mice. The DKO megakaryocytes did not display a significant defect in polyploidization under *in vitro* culture conditions (Figure 5E). This indicates that the lack of Cdk2 and Cdk4 does not affect homeostatic platelet counts, but impairs rapid platelet generation during recovery following stress. Next, we investigated the spleen for any changes in extramedullary hematopoiesis to determine whether there was a contribution to the phenotype in DKO mice. No significant change in the size of the spleen was noted (Figure 5F), and the fraction of various hematopoietic lineages tested in the spleen, except for orthochromatic erythroblasts which displayed a significant increase, remained unchanged in the DKO mice (Figure 5G-J). The proerythroblast fraction was slightly increased in the spleen but the difference was not statistically significant (Figure 5H). The mild increase in extramedullary erythropoiesis without significant changes in the other splenic lineages was consistent with the erythroid-specific abnormalities observed in the DKO mice under homeostatic conditions (Figure 1B). Finally, we checked whether deletion of Rb can rescue the defective platelet recovery after stress displayed by DKO mice (Figure 5B). Cdk2<sup>fl/fl</sup>Cdk4<sup>-/-</sup>Rb<sup>fl/fl</sup>vavCre (TKO) mice were defective in recovering their platelet counts following a 5-FU challenge, indicating that deletion of Rb is not sufficient to rescue the delayed recovery of platelet counts in the absence of Cdk2 and Cdk4 (Figure 5K).

In summary, we generated and characterized Cdk2<sup>fl/fl</sup>Cdk4<sup>-/-</sup>vavCre mice to demonstrate the specific overlapping functions of Cdk2 and Cdk4 during homeostatic and stress hematopoiesis. These findings, together with the hematopoietic defects reported in Cdk6<sup>-/-29</sup> and Cdk4<sup>-/-</sup>Cdk6<sup>-/-</sup> mice,<sup>7</sup> demonstrate that interphase Cdks have important unique and overlapping roles in mammalian hematopoiesis independent of their role in regulating proliferation. Although Cdk1 is sufficient for driving mammalian cell division,<sup>12</sup> interphase Cdks are critical for normal development. The proliferation of hematopoietic cells in the absence of Cdk2 and Cdk4 is most likely being driven by Cdk6 and Cdk1. While the critical requirement

for Cdk6 in mammalian hematopoiesis is well established,<sup>7,29</sup> the effect of specific inhibition of Cdk1 activity on hematopoiesis is not known. To this end, we crossed the Cdk1<sup>fl/fl</sup> mice<sup>16</sup> to vavCre mice. The Cdk1<sup>fl/fl</sup>vavCre mice were born at expected Mendelian ratios (25%; n=84) but died due to hematopoietic failure between postnatal days 1 and 4 (Figure 6A and B). The bone marrow cellularity was dramatically decreased in the neonatal Cdk1<sup>fl/fl</sup>vavCre mice (Figure 6C and D). Genotyping of peripheral blood indicated incomplete recombination of the floxed Cdk1 alleles, suggesting that the intact Cdk1 alleles enabled the Cdk1<sup>fl/fl</sup>vavCre mice to survive to birth (Figure 6E). Our data confirm the essential role of Cdk1 in hematopoiesis. These data highlight the potential deleterious effects on hematopoiesis upon use of broad spectrum Cdk inhibitors in therapy.

## Discussion

Although Cdks are central for driving proliferation, it is becoming increasingly apparent that their roles in development go beyond regulating the cell cycle and are often cell type specific.<sup>1</sup> We have previously demonstrated that combined loss of Cdk2 and Cdk4 leads to impaired S phase entry and premature senescence in MEFs,<sup>11</sup> but did not affect the cycling of neural stem cells.<sup>30</sup> Here we demonstrate that cycling of hematopoietic stem and progenitor cells (KSL) in the bone marrow, as well as the proliferation of purified fetal liver erythroblasts in culture, resemble neuronal stem cells in being unaffected by the loss of Cdk2 and Cdk4. The DKO mice displayed an increase in the erythrocyte MCV under homeostatic conditions, and the recovery of DKO platelet counts following stress was significantly delayed, revealing overlapping functions of Cdk2 and Cdk4 in mammalian hematopoiesis.

Regulators of the G1-S transition such as E2F4 and cyclin D-Cdk4/6 have been implicated in regulating erythrocyte size and/or numbers by controlling the number of erythroblast cell divisions during terminal differentiation.<sup>7,18-21</sup> E2F4<sup>-/-</sup> mice display fetal macrocytic anemia and enlarged adult erythrocytes due to late stage erythroblast maturation and proliferation defects.<sup>19-21</sup> Cdk6<sup>-/-</sup> mice display enlarged erythrocyte size accompanied by a concomitant decrease in erythrocyte counts and Cdk4<sup>-/-</sup>Cdk6<sup>-/-</sup> mice die during late gestation due to impaired erythropoiesis.<sup>7</sup> Loss of cyclin D3,<sup>18</sup> the major cyclin partner for Cdk4/6, phenocopies the enlarged erythroid cell size observed in Cdk6<sup>-/-</sup> and Cdk4<sup>-/-</sup>Cdk6<sup>-/-</sup> mice. Cyclin D3 regulates the erythrocyte size by regulating the number of cell divisions undergone by erythroblasts,<sup>18</sup> since the erythroid cell size gradually decreases during terminal proliferation and maturation of erythroblasts. Here we demonstrate that combined loss of Cdk2 and Cdk4 in erythroblasts results in increased erythrocyte size without affecting erythrocyte counts. Erythroblasts lacking Cdk2 and Cdk4 display a longer G1 phase of the cell cycle due to impaired phosphorylation of Rb. Since shortening of the G1 phase is critical for the normal progressive reduction in erythroid cell size during terminal differentiation,<sup>23</sup> we propose that the lengthened G1 phase of erythroblasts lacking Cdk2 and Cdk4 results in larger erythrocyte size. Further support for our model is provided by the genetic rescue of the increased erythrocyte size in mice

lacking Cdk2 and Cdk4 in the hematopoietic cells through the deletion of Rb, the gatekeeper of the G1-S transition and the phosphorylation target of Cdk2 and Cdk4. This demonstrates that the Cdk2/Cdk4/Rb pathway plays an important role in regulating erythrocyte size. Rb has previously been implicated in cell size checkpoint control in the unicellular alga *Chlamydomonas*.<sup>31</sup> Our data indicate that Rb is a critical component of the cell size checkpoint in mammalian cells.

Recovery of platelet counts following cytoablative stress is delayed in the absence of Cdk2 and Cdk4, revealing their important role during stress hematopoiesis. Although both Cdk2 and Cdk4 play critical roles in polyploidization of megakaryocytes that is essential for platelet generation,<sup>32-34</sup> only the platelet recovery following stress, but not the homeostatic platelet counts, were significantly affected in the absence of Cdk2 and Cdk4. This suggests that loss of Cdk2 and Cdk4 in megakaryocytes can be successfully compensated by other Cdks during homeostatic conditions (similar to the successful compensation observed in neuronal stem cells<sup>30</sup> lacking Cdk2 and Cdk4), but the compensation is inadequate for rapid proliferation and platelet gen-

eration following stress. These findings have important implications while considering the systemic use of broad-spectrum Cdk inhibitors in cancer therapy.

#### Acknowledgments

The authors would like to thank Vithya Anantaraja, Chloe Sim, and Zakiah Talib for animal care; the Biopolis shared facilities staff for flow cytometry services, and the Kaldis lab for support and discussions. We acknowledge the technical expertise provided by the Advanced Molecular Pathology Laboratory at IMCB.

#### Funding

This work was supported by the Biomedical Research Council of A\*STAR (Agency for Science, Technology and Research), Singapore.

#### Authorship and Disclosures

Information on authorship, contributions, and financial & other disclosures was provided by the authors and is available with the online version of this article at [www.haematologica.org](http://www.haematologica.org).

#### Reference

- Lim S, Kaldis P. Cdks, cyclins and CKIs: roles beyond cell cycle regulation. *Development*. 2013;140(15):3079-3093.
- Morgan DO. *The cell cycle: principles of control*. London: New Science Press Ltd; 2007.
- Malumbres M, Barbacid M. Cell cycle, CDKs and cancer: a changing paradigm. *Nat Rev Cancer*. 2009;9(3):153-166.
- Abate AA, Pentimalli F, Esposito L, Giordano A. ATP-noncompetitive CDK inhibitors for cancer therapy: an overview. *Expert Opin Investig Drugs*. 2013; 22(7):895-906.
- Malumbres M, Pevarello P, Barbacid M, Bischoff JR. CDK inhibitors in cancer therapy: what is next? *Trends Pharmacol Sci*. 2008;29(1):16-21.
- Berthet C, Aleem E, Coppola V, Tessarollo L, Kaldis P. Cdk2 knockout mice are viable. *Curr Biol*. 2003;13(20):1775-1785.
- Malumbres M, Sotillo R, Santamaria D, et al. Mammalian cells cycle without the D-type cyclin-dependent kinases Cdk4 and Cdk6. *Cell*. 2004;118(4):493-504.
- Ortega S, Prieto I, Odajima J, et al. Cyclin-dependent kinase 2 is essential for meiosis but not for mitotic cell division in mice. *Nat Genet*. 2003;35(1):25-31.
- Rane SG, Dubus P, Mettus RV, et al. Loss of Cdk4 expression causes insulin-deficient diabetes and Cdk4 activation results in islet cell hyperplasia. *Nat Genet*. 1999;22(5):44-52.
- Tsutsui T, Hesabi B, Moons DS, et al. Targeted disruption of CDK4 delays cell cycle entry with enhanced p27Kip1 activity. *Mol Cell Biol*. 1999;19(10):7011-7019.
- Berthet C, Klarmann KD, Hilton MB, et al. Combined loss of Cdk2 and Cdk4 results in embryonic lethality and Rb hypophosphorylation. *Dev Cell*. 2006;10(5):563-573.
- Santamaria D, Barriere C, Cerqueira A, et al. Cdk1 is sufficient to drive the mammalian cell cycle. *Nature*. 2007; 448(7155):811-815.
- Li W, Kotoshiba S, Berthet C, Hilton MB, Kaldis P. Rb/Cdk2/Cdk4 triple mutant mice elicit an alternative mechanism for regulation of the G1/S transition. *Proc Natl Acad Sci USA*. 2009;106(2):486-491.
- Georgiades P, Ogilvy S, Duval H, et al. vavCre transgenic mice: a tool for mutagenesis in hematopoietic and endothelial lineages. *Genesis*. 2002;34(4):251-256.
- Marino S, Vooijs M, van Der Gulden H, Jonkers J, Berns A. Induction of medulloblastomas in p53-null mutant mice by somatic inactivation of Rb in the external granular layer cells of the cerebellum. *Genes Dev*. 2000;14(8):994-1004.
- Diril MK, Ratnacaram CK, Padmakumar VC, et al. Cyclin-dependent kinase 1 (Cdk1) is essential for cell division and suppression of DNA re-replication but not for liver regeneration. *Proc Natl Acad Sci USA*. 2012;109(10):3826-3831.
- Jayapal SR, Lee KL, Ji P, Kaldis P, Lim B, Lodish HF. Down-regulation of Myc is essential for terminal erythroid maturation. *J Biol Chem*. 2010;285(51):40252-40265.
- Sankaran VG, Ludwig LS, Sicinska E, et al. Cyclin D3 coordinates the cell cycle during differentiation to regulate erythrocyte size and number. *Genes Dev*. 2012;26(18):2075-2087.
- Humbert PO, Rogers C, Ganiatsas S, et al. E2F4 is essential for normal erythrocyte maturation and neonatal viability. *Mol Cell*. 2000;6(2):281-291.
- Kinross KM, Clark AJ, Iazzolino RM, Humbert PO. E2f4 regulates fetal erythropoiesis through the promotion of cellular proliferation. *Blood*. 2006;108(3):886-895.
- Rempel RE, Saenz-Robles MT, Storms R, et al. Loss of E2F4 activity leads to abnormal development of multiple cellular lineages. *Mol Cell*. 2000;6(2):293-306.
- Hattangadi SM, Wong P, Zhang L, Flygare J, Lodish HF. From stem cell to red cell: regulation of erythropoiesis at multiple levels by multiple proteins, RNAs, and chromatin modifications. *Blood*. 2011;118(24):6258-6268.
- Dolznic H, Bartunek P, Nasmyth K, Mullner EW, Beug H. Terminal differentiation of normal chicken erythroid progenitors: shortening of G1 correlates with loss of D-cyclin/cdk4 expression and altered cell size control. *Cell Growth Differ*. 1995;6(11):1341-1352.
- Nowakowski RS, Lewin SB, Miller MW. Bromodeoxyuridine immunohistochemical determination of the lengths of the cell cycle and the DNA-synthetic phase for an anatomically defined population. *J Neurocytol*. 1989;18(3):311-318.
- Ji P, Jayapal SR, Lodish HF. Enucleation of cultured mouse fetal erythroblasts requires Rac GTPases and mDia2. *Nat Cell Biol*. 2008;10(3):314-321.
- Zhang J, Socolovsky M, Gross AW, Lodish HF. Role of Ras signaling in erythroid differentiation of mouse fetal liver cells: functional analysis by a flow cytometry-based novel culture system. *Blood*. 2003;102(12):3938-3946.
- Herrera RE, Sah VP, Williams BO, Makela TP, Weinberg RA, Jacks T. Altered cell cycle kinetics, gene expression, and G1 restriction point regulation in Rb-deficient fibroblasts. *Mol Cell Biol*. 1996;16(5):2402-2407.
- Weinberg RA. The retinoblastoma protein and cell cycle control. *Cell*. 1995;81(3):323-330.
- Hu MG, Deshpande A, Enos M, et al. A requirement for cyclin-dependent kinase 6 in thymocyte development and tumorigenesis. *Cancer Res*. 2009;69(3):810-818.
- Lim S, Kaldis P. Loss of Cdk2 and Cdk4 induces a switch from proliferation to differentiation in neural stem cells. *Stem Cells*. 2012;30(7):1509-1520.
- Fang SC, de los Reyes C, Umen JG. Cell size checkpoint control by the retinoblastoma tumor suppressor pathway. *PLoS Genet*. 2006;2(10):e167.
- Datta NS, Williams JL, Long MW. Differential modulation of G1-S-phase cyclin-dependent kinase 2/cyclin complexes occurs during the acquisition of a polyploid DNA content. *Cell Growth Differ*. 1998;9(8):639-650.
- Kilbey A, Alzuherri H, McColl J, et al. The Evi1 proto-oncoprotein blocks endomitosis in megakaryocytes by inhibiting sustained cyclin-dependent kinase 2 catalytic activity. *Br J Haematol*. 2005;130(6):902-911.
- Muntean AG, Pang L, Poncz M, et al. Cyclin D-Cdk4 is regulated by GATA-1 and required for megakaryocyte growth and polyploidization. *Blood*. 2007; 109(12):5199-5207.